J. Physiol. (1984), **354**, *pp.* 605–624
With 7 text-figures
Printed in Great Britain

INITIATION OF ACTIVE CONTRACTION BY PHOTOGENERATION OF ADENOSINE-5′-TRIPHOSPHATE IN RABBIT PSOAS MUSCLE FIBRES

BY Y. E. GOLDMAN*, M. G. HIBBERD* AND D. R. TRENTHAM†

From the Department of Physiology and the Department of Biochemistry and Biophysics†, University of Pennsylvania, Philadelphia, PA 19104, U.S.A.*

(*Received 6 December 1983*)

SUMMARY

1. Mechanical and biochemical descriptions of the muscle cross-bridge cycle have been correlated. Skinned muscle fibres of rabbit psoas muscle in rigor were incubated in solutions containing ≈ 30 μM-Ca^{2+} ions and P^3-1-(2-nitro)phenylethyladenosine-5′-triphosphate, 'caged ATP', an inert photolabile precursor of ATP. ATP was liberated from caged ATP within the fibres by pulses of 347 nm radiation from a frequency-doubled ruby laser. The mechanical responses of muscle fibres to the rapid increase of ATP concentration were monitored.

2. Tension dropped briefly and then rose above the rigor value to the level characteristic of a steady active contraction. Liberation of ATP decreased in-phase stiffness (measured at 500 Hz) from the rigor level to a maintained value intermediate between rigor and relaxed values. Out-of-phase stiffness increased to a maintained level indicating a phase lead of tension with respect to imposed length oscillations.

3. Rigor tension was varied prior to photolysis by slight alterations of fibre length. Tension traces starting at different rigor tensions converged to a common tension level at the same rate, whether or not Ca^{2+} was included in the medium. These data suggest that the rate of cross-bridge detachment by ATP from the rigor state is not influenced by Ca^{2+}.

4. Analysis of the tension records, in terms of sequential detachment and re-attachment reactions, provided a measure of cross-bridge reattachment rate and an alternate measure of the detachment rate. Detachment from the rigor state was approximately proportional to the ATP concentration, with a second-order rate constant of at least 5×10^5 M^{-1} s^{-1}. Reattachment with force generation had no detectable dependence on the concentration of ATP liberated by photolysis.

5. A simple kinetic model of the cross-bridge cycle in terms of chemically defined intermediates was compatible with most of the experimental data. The ATP dependence of cross-bridge detachment, the kinetics of maintained cross-bridge reattachment in the presence of Ca^{2+}, and transient reattachment and final relaxation in the absence of Ca^{2+} were explained. In this model, reversibility of cross-bridge attachment and the steps leading to force production allow the relatively high observed detachment rate to be accommodated with other data relating to active contraction. These data include the steady ATPase rate of active muscle fibres and the fewer attached cross-bridges in active contractions compared to rigor.

INTRODUCTION

An evaluation of the rates of the elementary mechanical and biochemical reactions in the cyclic interaction between actin and myosin is an essential requirement for a quantitative description of the cross-bridge theory of muscle contraction (A. F. Huxley, 1957; Podolsky & Nolan, 1973; Julian, Sollins & Sollins, 1974; Eisenberg, Hill & Chen, 1980; Steiger & Abbott, 1981; Thorson & White, 1983). Cross-bridge attachment rate influences the force, the number of attachments, and the control of energy liberation as the load is varied. This rate can be inferred from the rate of tension or stiffness increase when a muscle is activated (Cecchi, Griffiths & Taylor, 1982) or abruptly allowed to shorten (A. F. Huxley, 1974), and from time-resolved X-ray diffraction experiments in which the movement of mass from the thick toward the thin filaments is monitored (Matsubara & Yagi, 1978; H. E. Huxley, 1979). These methods provide lower limits for the cross-bridge attachment rate, because other phenomena (such as the release of Ca^{2+} and its binding to troponin) may limit the transient development of tension or stiffness in these experiments.

We have previously shown that rapid photochemical liberation of ATP within a skinned muscle fibre in the presence of Ca^{2+} ions switches the contractile apparatus from rigor to an active contraction without an intermediate full relaxation (Goldman, Hibberd, McCray & Trentham, 1982). The rapid onset of active force was interpreted as an indication that, after detachment by ATP, cross-bridges re-form at a rate comparable to the detachment rate. The results suggest that little rate limitation of the cross-bridge cycle occurs in the segment of the reaction pathway where myosin is dissociated from actin, assuming that ATP detaches cross-bridges in the presence of Ca^{2+} ions.

In the present experiments, muscle fibres were switched from rigor to active contraction by laser pulse photolysis of P^3-1-(2-nitro)phenylethyladenosine-5′-triphosphate ('caged ATP'), within the muscle fibre filament lattice in the presence of Ca^{2+} ions. The kinetics of transient tension and stiffness changes were investigated to obtain estimates of cross-bridge detachment and reattachment rates. The assumption that ATP detaches cross-bridges in the presence of Ca^{2+} was tested by observing convergence of tension traces when ATP was released with the fibre bearing various rigor tensions. Cross-bridge detachment rate was not appreciably altered by the presence or absence of Ca^{2+} ions, but was markedly dependent on the ATP concentration. Reattachment rate had little or no dependence on ATP concentration. A simple kinetic model of the cross-bridge cycle, consistent with the mechanism of ATP hydrolysis by actomyosin in solution, can explain most of the results.

METHODS

The laser photolysis technique used for analysing the effects of quick changes in ATP concentration within skinned muscle fibres and the recording instrumentation were described in the preceding paper (Goldman, Hibberd & Trentham, 1984). As in earlier studies, we used both mechanically and chemically skinned single-fibre preparations of rabbit psoas muscle. No consistent difference in the mechanical properties of the two types of fibres was observed. Chemically skinned fibres were stored in 50% glycerol solutions and kept at −22 °C for up to 6 weeks. The solutions used in the experiments are listed in Table 1 except where noted in the text.

Experimental protocol. Tension and in-phase stiffness recordings (Fig. 1) show the sequence of

TABLE 1. Solutions used during caged ATP photolysis trials

	Mg ATP	$MgCl_2$	Mg^{2+}	EGTA	Ca^{2+}	$K^+ + Na^+$	TES	CP	CK†	GSH	Caged ATP
Rigor	0	3·2	1	53	*	140	100	0	0	10	0
Rigor with CP	0	2·6	1	30	*	138	100	22	1	10	0–10
Rigor with Ca^{2+}	0	1·3	1	30‡	0·03	138	100	22	1	10	0–10
0·1 mM-ATP relax	0·1	2·7	1	30	*	138	100	22	1	10	0
5·0 mM-ATP relax	5·0	7·4	1	30	*	141	100	11	0	10	0

* $Ca^{2+} < 10^{-8}$ M.

† mg ml^{-1} 100–150 units activity: one unit transfers 1·0 μmol phosphate from CP to ADP per minute at pH 7·4 and 30 °C (Sigma Chemical Co.).

‡ CaEGTA.

All concentrations mM unless stated otherwise. Over-all ionic strength of the solutions was 0·2 M. Solutions were made up at room temperature (20–22 °C) and brought to pH 7·1 with KOH or HCl.

EGTA ethyleneglycol-*bis*-(β-aminoethylether)-*N*,*N*,*N*′,*N*′-tetraacetic acid.

TES *N*-Tris(hydroxymethyl)methyl-2-aminoethanesulphonic acid.

GSH glutathione (reduced form).

CP creatine phosphate.

CK creatine kinase.

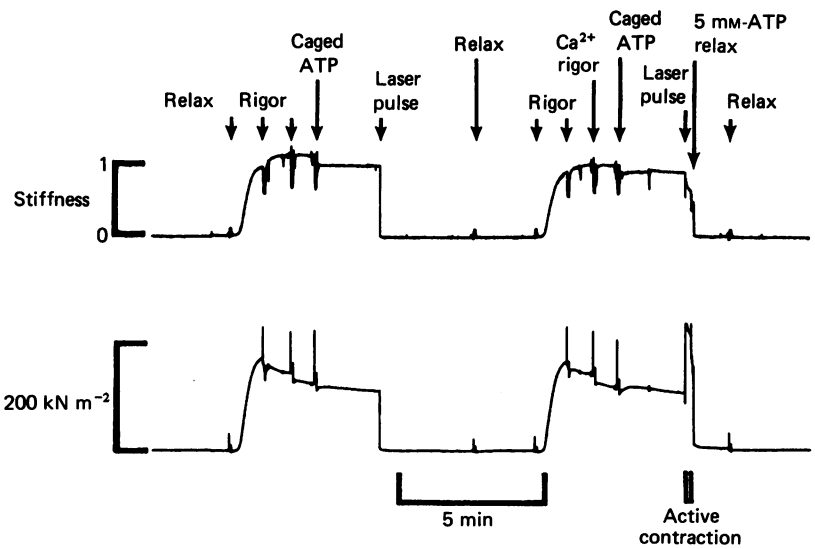

Fig. 1. Protocol for initiation of mechanical transients by liberation of ATP within a single rigor muscle fibre in the absence and presence of Ca^{2+}. Slow time-base chart records of in-phase stiffness (upper) and tension (lower) during two successive rigor–photolysis trials. The composition of the bathing medium around the fibre was changed at the times indicated by arrows labelled with the new solution. Initial caged ATP was 10 mM, free Mg^{2+} was 2 mM. Final ATP concentration: 500 μM. Fibre dimensions: 1·84 mm × 4215 μm^2; sarcomere length = 2·27 μm; T = 20·0 °C.

events in two successive rigor–photolysis trials. The muscle fibre was initially immersed in a 100 μM-Mg ATP relaxing solution (Table 1). The solution surrounding the fibre was exchanged for a rigor solution without creatine phosphate (CP; Table 1). The bathing medium was changed to a rigor solution containing CP and creatine kinase (CK), and then caged ATP solution at the times indicated. A time of 2 min was allowed for caged ATP to diffuse into the filament lattice. A pulse from a frequency-doubled ruby laser released ATP from the caged ATP and the fibre rapidly

relaxed. The fibre was put into 100 μM-Mg ATP relaxing solution at the point labelled 'Relax' in Fig. 1. During the next rigor contraction the rigor+CP and caged ATP solutions contained approximately 30 μM-free Ca^{2+}. The addition of Ca^{2+} to the rigor solution caused little alteration of rigor force or stiffness. Addition of caged ATP caused a slight decrease in force and stiffness in the presence and absence of Ca^{2+}. This effect of caged ATP before photolysis is discussed by Goldman *et al.* (1984) and Ferenczi, Homsher & Trentham (1984).

When the laser pulse released ATP in the presence of Ca^{2+}, the force approximately doubled and stiffness decreased to about 70% of the rigor value (Fig. 1). After 10–20 s of active contraction, the fibre was relaxed by exchanging the solution for a 5 mM-Mg ATP, Ca^{2+}-free relaxing solution (Table 1).

In some experiments a small length change was applied 1 s before the laser pulse to alter the distribution of stress in the rigor cross-bridges. The final ATP concentration was varied by altering the intensity of the laser pulse. Further details of the solution exchange apparatus and assay for ATP release have been described by Goldman *et al.* (1984). In the protocol for the present experiments two solution exchanges with Ca^{2+} were found to be necessary to obtain reproducible active tension values, presumably by washing out free EGTA from the fibre and the trough.

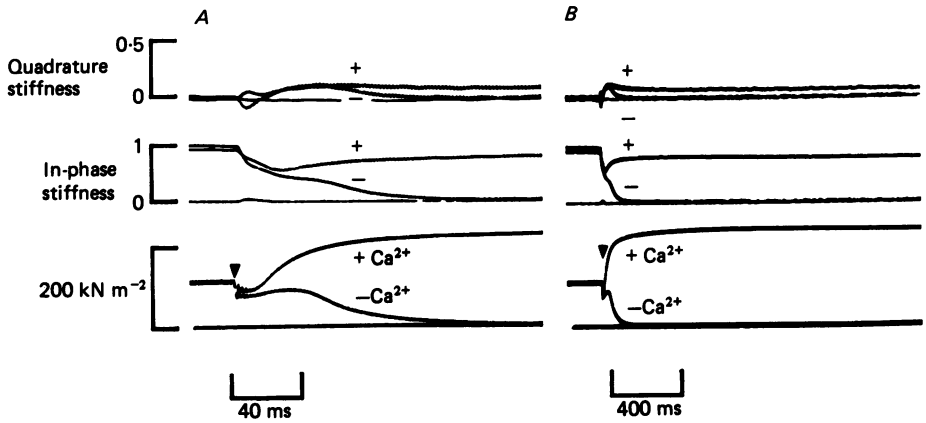

Fig. 2. Stiffness and tension transients induced by liberation of ATP. *A* and *B* represent fast and slow time-base oscilloscope records of quadrature stiffness (upper traces), in-phase stiffness (centre), and tension (lower) during the experimental trials illustrated in Fig. 1. Records obtained with or without added Ca^{2+} are labelled + and − respectively. Arrows mark the time at which the laser pulse was triggered. Base lines were obtained about 1 min after relaxation had been completed. All the records show transient artifacts induced directly by the laser pulse, apparent as a 'step' decrease in the tension records and the longer-lived (5–10 ms) artifacts at the beginning of the stiffness records (particularly quadrature stiffness). Other details were as listed in the legend of Fig. 1.

RESULTS

Photolysis in the presence and absence of Ca^{2+}. The results of releasing ATP rapidly into a rigor fibre in the presence (+) and absence (−) of free Ca^{2+} are compared in Fig. 2. The transient features of the mechanical response to liberation of ATP in the absence of Ca^{2+} were described previously (Goldman *et al.* 1982, 1984). Briefly, tension decreases as ATP detaches rigor cross-bridges, then it increases due to transient cross-bridge reattachment and finally falls to the relaxed level. In-phase stiffness decays continuously after the laser pulse. Out-of-phase (quadrature) stiffness increases transiently and then decays. With Ca^{2+} present, release of ATP was followed by a

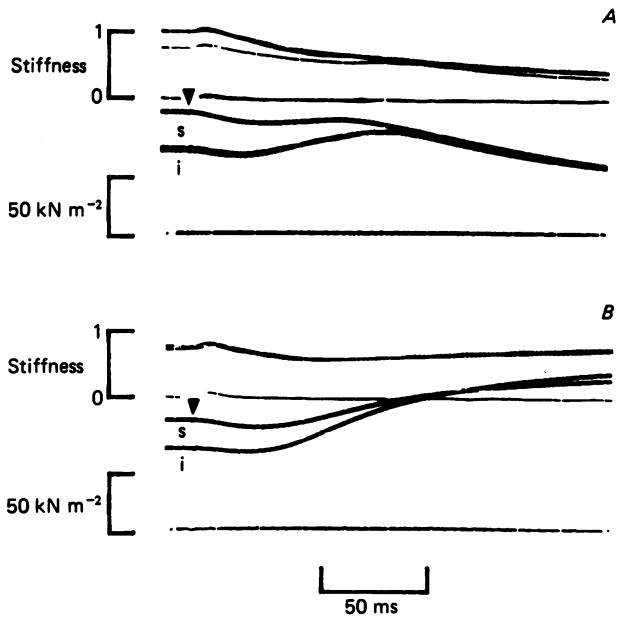

Fig. 3. Convergence of tension records in the presence and absence of Ca^{2+}. Superimposed in-phase stiffness (upper) and tension (lower) records from successive photolysis trials conducted with a single fibre. Each panel shows an isometric record (i) and a recording after a pre-stretch (s) of 0·61 % applied 1 s before the laser pulse. Initial caged ATP concentration was 10 mM. *A*, no added Ca^{2+}. Final ATP concentrations were 96 μM (i) and 118 μM (s). Base-line levels were recorded in the photolysis solution after relaxation. The upper stiffness trace corresponds to the pre-stretch tension record. Splitting of the stiffness traces is an indication of non-linearity of the fibre force–extension curve. *B*, $\approx$30 μM-free Ca^{2+}. Final ATP concentrations were 196 μM (i) and 161 μM (s). Base-line levels were obtained about 1 min after relaxation in a 5 mM-Mg ATP relaxing solution. Fibre dimensions: 2·73 mm × 5081 μm^2; sarcomere length = 2·66 μm, T = 20·3 °C.

brief decrease of tension (lower traces) and then an increase to the steady contraction. The tension traces recorded in the presence and absence of Ca^{2+} were separated 15 ms after the laser pulse, indicating that Ca-dependent force generation occurred shortly after ATP bound to the rigor cross-bridges.

The in-phase stiffness (Fig. 2, middle traces) decreased from the rigor level and, in the absence of Ca^{2+}, continued to decline to the relaxed level. In the presence of Ca^{2+}, stiffness decreased briefly and then increased to a final level below the rigor value. The time at which the minimum stiffness occurred was later than the time of minimum tension. The stiffness traces recorded in the presence and absence of Ca^{2+} separated later (20–30 ms after the laser pulse) than the tension traces.

Quadrature (out-of-phase) stiffness was set to zero in the rigor solution before the laser pulse by adjusting the phase angle of the demodulation reference signal (Goldman *et al.* 1984). The quadrature signal began to rise about 10 ms after the laser pulse, indicating a phase lead of tension with respect to the sinusoidal length change. The phase lead, indicating the presence of active cross-bridges with quick stress relaxation (Kawai & Brandt, 1980), was maintained in the presence of Ca^{2+}, but

decayed back to zero in Ca^{2+}-free conditions. The deflexion of the quadrature signals in Fig. 2, within the first 5 ms after the laser pulse, was an artifact related to feed-through of non-sinusoidal tension components in the lock-in amplifier used to demodulate the stiffness signals.

Tension difference trace. The tension increment produced by a pre-photolysis length change would be expected to decay at the rate of the first ATP-induced detachment of the rigor cross-bridges, if the force generated by reattached cross-bridges was independent of the length change (Goldman *et al.* 1984). The rate of convergence of tension traces starting at different rigor tensions would then indicate detachment kinetics unmodified by subsequent cycling and force generation. Fig. 3 shows records from an experiment in which the convergence of tension traces, starting at different rigor tensions, was compared in the absence (panel *A*) and presence (panel *B*) of Ca^{2+}. Each panel shows an isometric trial (i) and a trace recorded when the fibre was stretched in rigor shortly before the laser pulse (s). The convergence of the two pairs of traces occurred at almost the same rate, indicating that Ca^{2+} did not affect the rate of detachment of rigor cross-bridges induced by ATP

Variation of ATP concentration. The transient and steady-state tension and stiffness signals were all influenced by the final concentration of ATP liberated by photolysis. Fig. 4 shows a series of photolysis trials in the presence of Ca^{2+} at various final ATP concentrations. Two records are superimposed in each panel: an isometric trial (i) and a pre-stretch trial (s). The tension traces in each panel converged more rapidly at higher ATP concentration (*A*) than at lower concentrations (*C* and *E*). These results indicate that cross-bridge detachment from the rigor state is dependent on the ATP concentration in the presence of Ca^{2+} ions.

The in-phase stiffness decreased after the laser pulse to a value intermediate between the rigor and the relaxed levels. Steady active stiffness was a smaller proportion of the rigor stiffness at the higher ATP concentrations. The maintained component of quadrature stiffness after ATP release had a greater amplitude at higher ATP concentrations (Fig. 4*A* and *B*) compared to the lower ATP concentrations (Fig. 4*C–F*). The phase lead of the sinusoidal tension signal with respect to the length oscillation was $19{\cdot}6 \pm 1{\cdot}8$ deg (mean $\pm$ S.E. of mean, $n = 22$) at 450 ± 46 μM-Mg ATP and $5{\cdot}3 \pm 0{\cdot}8$ deg (mean $\pm$ S.E. of mean, $n = 10$) at 51 ± 7 μM-Mg ATP. When ATP was released, tension decreased and then rose to a steady active level. The transient decrease of tension was greater for the pre-stretch trials (s) than for the isometric trials (i). At the higher ATP concentrations the amplitude of this transient decrease was greater and the minimum tension value occurred earlier than at the lower ATP concentrations. The results shown in Fig. 4 were typical of experiments on thirteen fibres.

Kinetic analysis. These observations are consistent with a working hypothesis in which the tension decrease represents transient detachment of rigor cross-bridges followed by reattachment and formation of an active force-generating state. This sequence is indicated by the following scheme:

$$\text{Rigor} \xrightarrow{k_d} \text{Detached} \xrightarrow{k_r} \text{Active}$$

in which the 'detached state' produces no force and the 'active' cross-bridge state includes all of the intermediates of the active cross-bridge cycle. If first-order kinetics

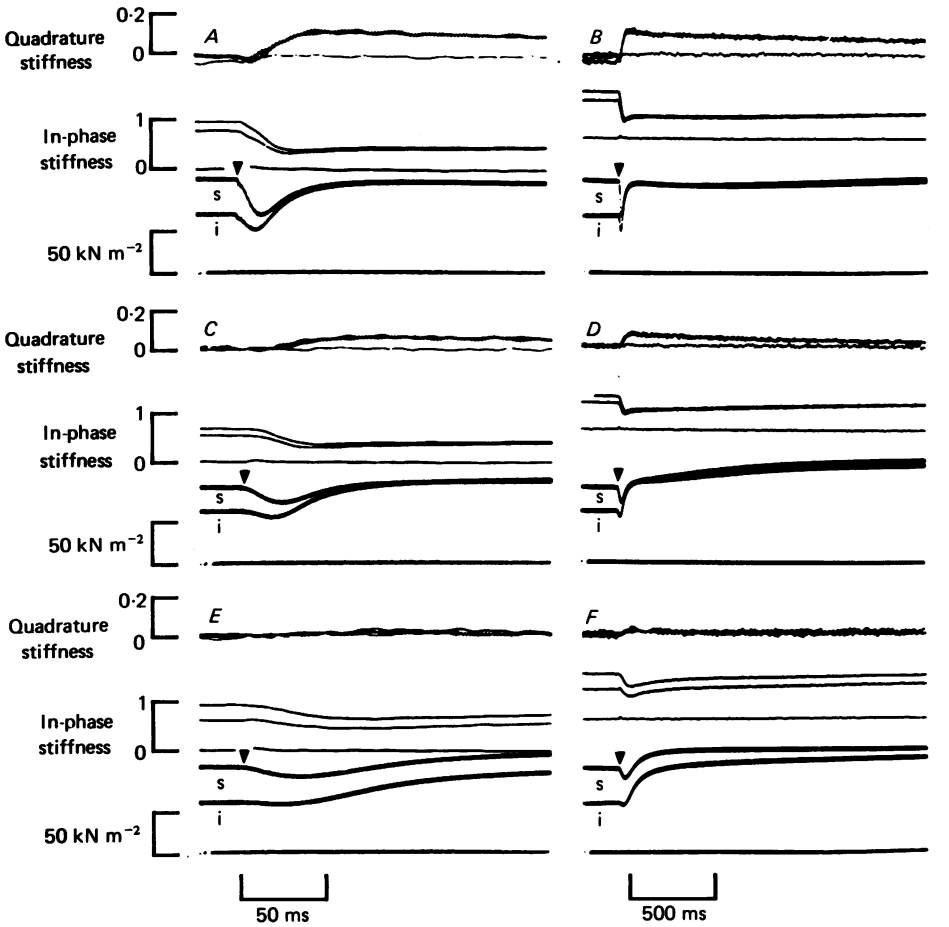

Fig. 4. Effect of altering the concentration of liberated ATP in the presence of Ca^{2+}. Paired fast (*A*, *C* and *E*) and slow (*B*, *D* and *F*) time-base recordings of force (lower) and stiffness (centre and upper). ATP concentration was altered by varying the laser pulse energy. Each panel shows superimposed records from two successive trials at each laser intensity: an isometric trial (i) and trial after a 0·74 % pre-stretch (s). Muscles were initially in the rigor state with 30 μM-Ca^{2+} and 10 mM-caged ATP. The laser was triggered at the points marked by the arrows. Base lines were recorded in a 5 mM-Mg ATP relaxing solution about 1 min after relaxation. The final ATP concentrations were: *A* and *B*, 520 μM; *C* and *D*, 169 μM; *E* and *F*, 51 μM. Fibre dimensions: 2·24 mm × 4604 μm^2; sarcomere length = 2·30 μm, T = 20·2 °C.

are assumed for the detachment reaction and for reattachment with force generation, the force expected after the release of ATP is given by:

$$\frac{T}{T_0} = F.\exp(-k_d t)+1-\frac{k_r}{k_r-k_d}\exp(-k_d t)-\frac{k_d}{k_d-k_r}\exp(-k_r t), \quad (1)$$

where T/T_0 = relative force as a function of time (t), F = the fraction of active force present in the rigor state at the time of the laser pulse, k_d = rate of detachment, and k_r = rate of reattachment into the active force-generating state.

An iterative technique (McCalla, 1967) was used to find values of k_d and k_r that

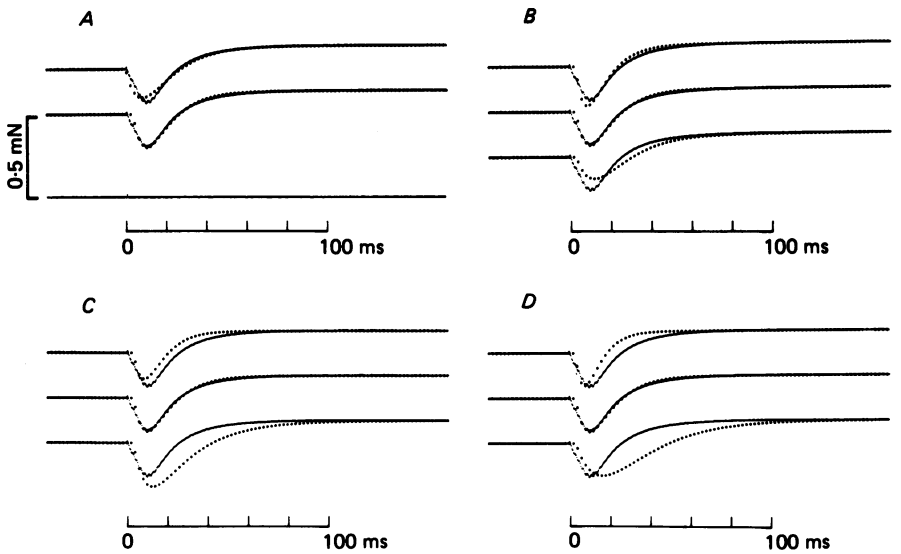

Fig. 5. Computer fits to tension transients in the presence of Ca^{2+}. An experimental data trace is repeated in each panel (continuous line). A single fibre was in rigor and equilibrated with caged ATP and 30 μM-Ca^{2+} at the start of the experimental record. The laser was triggered at the time indicated by a decrease in tension. 779 μM-ATP was liberated by photolysis. T = 20·3 °C. Tension transients predicted by eqn. (1) are shown by the dotted traces, with a 2 ms interval between plotted points. *A*, upper, time-zero point for the simulation coincided with the time of the laser pulse. k_d and k_r in eqn. (1) were 106 and 89 s^{-1}. Lower, time-zero point for eqn. (1) was shifted 3·6 ms later than the laser pulse to adjust for the finite rate of formation of ATP from caged ATP. k_d = 150 s^{-1}; k_r = 100 s^{-1}. The flat lower trace represents the tension base line appropriate for the lower of the pair of transients, together with the tension calibration bar. Rate constants (k_d and k_r, s^{-1}) for simulated traces in the other panels were respectively: *B*, upper 225, 100; centre 150, 100; lower 75, 100; *C*, upper 150, 150; centre 150, 100; lower 150, 50; *D*, upper 225, 150; centre 150, 100; lower 75, 50.

minimized the sum of the squares of tension differences (residuals) between eqn. (1) and observed tension records. F was measured directly from each tension record. If the time-zero point in eqn. (1) was made to coincide with the time of the laser pulse, then a consistent deviation of eqn. (1) from the tension recording was observed. Fig. 5*A* shows the tension record (upper trace) from an experiment in which 779 μM-ATP was released in the presence of Ca^{2+}. The heavier dots are tension values predicted by eqn. (1) for values of k_d and k_r which minimize the sum of the squared residuals. The tension predicted by eqn. (1) decreased more rapidly than the recorded tension, reached minimum tension earlier, and rose above the recorded tension at the time of minimum force. The tension minimum given by eqn. (1) occurred before the observed tension minimum, indicating that fibre tension initially declined less rapidly than expected on the basis of a first-order detachment reaction. A delay of detachment is expected from the photochemical dark reactions which control ATP release at about 100 s^{-1} after caged ATP absorbs a photon. In addition, ATP binding to cross-bridges reduced the free ATP concentration within the fibres during the transients, and this factor also slowed detachment. An empirical approach was taken

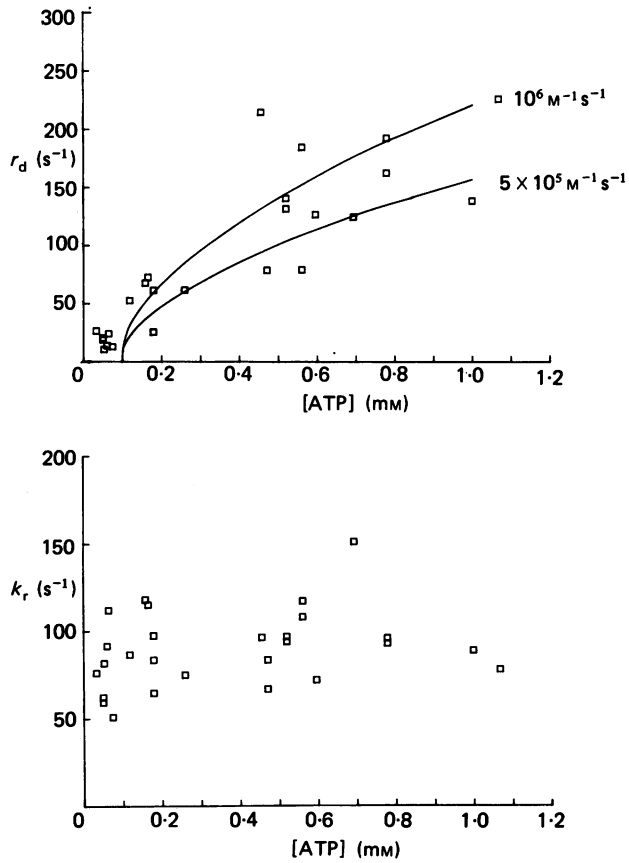

Fig. 6. ATP dependence of cross-bridge detachment and reattachment rates in the presence of Ca^{2+}. *A*, cross-bridge detachment rate determined by fitting eqn. (1) of the text to tension transients are plotted as reciprocal half-times ($r_d = k_d/0{\cdot}693$) *vs.* final ATP concentration. The lines represent the expected convergence rate, taking into account photolysis dark reactions limiting ATP release to 100 s^{-1}, a 200 μM-myosin head concentration, and two second-order rate constants for the ATP-induced dissociation of cross-bridges as labelled. *B*, rate constant k_r for reattachment of cross-bridges as determined from fitting eqn. (1) to tension transients.

to account for these factors in the quantitative analysis. The parameters k_d and k_r were recalculated after shifting the time-zero point of eqn. (1) by 3·6 ms so that the predicted time of minimum tension coincided with the observed minimum. This time shift considerably improved the correspondence between eqn. (1) and the observed tension (Fig. 5*A*, centre trace). A consistent deviation between the calculated and the observed tension then only occurred during the first few milliseconds after the laser pulse.

Fitting eqn. (1) to the tension data gave distinct values for both k_d and k_r, as illustrated by Fig. 5*B–D*. In panel *B*, k_d was varied $\pm 50\%$ about the optimum value (shown as the centre curve), and deviations were observed in the tension minimum and time course of the approach to the active force level. In panel *C*, k_r was varied

$\pm 50\%$ from the optimum value, and deviations between eqn. (1) and the tension trace were again observed. In panel *D*, k_d and k_r were both varied $\pm 50\%$, but the ratio k_d/k_r was held constant. In this case the amplitude of the initial tension decrease predicted by eqn. (1) was constant, but the time to the tension minimum and the approach to the steady contraction level differed from the tension recording. Thus, both k_d and k_r had to be optimized to fit eqn. (1) to a tension trace.

A series of twenty-seven tension traces from thirteen muscle fibres was analysed to find the values of k_d and k_r that provided the best fits to records obtained over a range of final ATP concentrations. The results were plotted as reciprocal half-times ($r_d = k_d/0{\cdot}693$) *vs.* final ATP concentration (Fig. 6*A*). The r_d values were increased as the ATP concentration was raised, indicating that the initial cross-bridge detachment was ATP dependent. The curves drawn in Fig. 6*A* represent expected half-times for cross-bridge detachment calculated as described by Goldman *et al.* (1984). The rate constant of ATP release from irradiated caged ATP was assumed to be $100\ s^{-1}$ and the myosin head concentration in the muscle fibre was taken as $200\ \mu M$. The data fall in the range expected for a second-order rate constant for cross-bridge detachment by ATP between 5×10^5 and $10^6\ M^{-1}\ s^{-1}$. These values are in the same range as the second-order constant for cross-bridge detachment in the absence of Ca^{2+} (Goldman *et al.* 1984).

The apparent rates of cross-bridge reattachment (k_r) determined from fitting eqn. (1) to tension traces were plotted *vs.* ATP concentration in Fig. 6*B*. There was no significant dependence of k_r on ATP concentration. Taking all ATP concentrations together, the rate of cross-bridge reattachment was $83 \pm 4\ s^{-1}$ (mean $\pm$ S.E. of mean, $n = 27$).

DISCUSSION

Cross-bridge detachment and reattachment rates. The rate of ATP-induced cross-bridge detachment from rigor has been measured by two separate mechanical properties of muscle fibres. First, the detachment rate was estimated from the rate of decay of the extra tension produced by stretching muscle fibres shortly before photolytic release of ATP. This decay occurs at a similar rate in the presence and absence of Ca^{2+} (Fig. 3). Secondly, cross-bridge detachment rate was determined by fitting the time course of tension in the presence of Ca^{2+} to a simple detachment–reattachment scheme. Estimates of cross-bridge detachment rate from these two methods of analysis were the same ($>5 \times 10^5\ M^{-1}\ s^{-1}$) over a range of ATP concentrations and in the presence or absence of Ca^{2+}. Two aspects of detachment, (1) loss of the effect of previously imposed distortion (Figs. 3 and 4 and Goldman *et al.* 1984), and (2) decreased force (Figs. 5 and 6), apparently occur at the same rate.

An early decrease of tension before a force increase was previously observed in the absence of Ca^{2+} ions (Goldman *et al.* 1982, 1984). However, the subsequent mechanical transients in the absence of Ca^{2+} were complex, so that a description required several parameters. In contrast, the force transient which occurs in the presence of Ca^{2+} ions is described adequately by two serial first-order processes and an analytical expression (eqn. (1) and Fig. 5). For given initial rigor and final active tensions, the magnitude of the transient tension decrease, predicted by eqn. (1), depends only on the ratio of the detachment rate (k_d) to the subsequent reattachment rate (k_r, Fig. 5).

Therefore, the greater amplitude of the transient tension decrease at higher ATP concentration (Fig. 4) is evidence that reattachment depends less on ATP than detachment. Numerical estimates of the reaction rates (k_d and k_r) required to fit the experimental data show a strikingly different dependence on ATP concentration (Fig. 6). While cross-bridge detachment (k_d) depends strongly on ATP concentration, the reaction leading to increased force (k_r) has little if any ATP dependence. These observations provide evidence that the initial decrease of force is related to ATP binding and the increasing force is controlled by a subsequent first-order step.

When ATP detaches a cross-bridge, the myosin head might reattach to the same actin monomer or to another site on the thin filament. Geometric constraints of the filament lattice, occupation of thin filament sites by other cross-bridges, or a high reattachment rate compared to the rate of axial cross-bridge motion might cause the cross-bridge to reattach to its original actin binding site. The reattachment would then retain the distortion and force imposed by a pre-stretch or pre-release. However, if the site of reattachment is not biased by the position of the original site or by the pre-photolysis length change, then cross-bridges originally bearing high levels of force and corresponding structural distortion would tend to find reattachment positions with lower free energy and lower force. Thus a rapidly reversible detachment with reattachments independent of the pre-stretch is also consistent with our results.

Since the kinetic analysis was performed on force records, the procedure measured the rate of force production of cross-bridges after being detached, rather than reattachment. The existence of an initial cross-bridge attachment state with low force has been inferred from observations of the equatorial X-ray diffraction pattern during the rising phase of intact muscle contractions (H. E. Huxley, 1979; Matsubara & Yagi, 1978) and from stiffness measurements made during the rising phase of active muscle fibre twitches (Cecchi *et al.* 1982). If cross-bridges reattach to form an initial state producing little force and then generate force after a separate step, the data indicate that the over-all rate of reattachment and force generation occurs at 50–100 s^{-1}.

Stiffness recordings. If the stiffness per attachment is independent of the state of the cross-bridge, then stiffness measurements might distinguish the attachment from the step leading to force production. In Ca^{2+}-containing solutions, the in-phase stiffness decreased after the laser pulse and then usually increased slightly to the level maintained during the steady active contraction. However, the increase in stiffness may be an artifact due to non-linearity of the fibre's force–extension curve. This non-linearity is evident as an increase in apparent stiffness when a fibre is stretched in rigor (upper stiffness traces in Figs. 3 and 4; Goldman *et al.* 1984, Fig. 2). Presence of this non-linearity would contribute to the increase in stiffness during the rise in tension in Figs. 2 ($+Ca^{2+}$), 3*B* and 4. On the other hand, the decrease in stiffness during the rising tension phase and the steady decrease compared to the rigor value would not be caused by this non-linearity. The decreased in-phase stiffness during Ca^{2+}-activated contractions compared to the rigor stiffness suggests that fewer cross-bridge attachments exist during active contraction than in the rigor state. This conclusion is consistent with stiffness measurements in other tissues (Goldman & Simmons, 1977; Yamamoto & Herzig, 1978) and with X-ray diffraction data

(Haselgrove & Huxley, 1973; Matsubara, Yagi & Hashizume, 1975). The quadrature stiffness signals indicate the presence of cross-bridges with viscoelastic behaviour corresponding to the quick stress relaxation observed in length-step experiments (Ford, Huxley & Simmons, 1977; Kawai & Brandt, 1980). The maintained quadrature stiffness in the presence of Ca^{2+} is similar in magnitude to the transient quadrature stiffness which develops during relaxation after caged ATP photolysis in the absence of Ca^{2+} (Fig. 2). This finding suggests that a substantial proportion of cross-bridges reattach to the actin even in the absence of Ca^{2+} (see also Goldman *et al.* 1984).

The magnitude of the quadrature stiffness can be used to estimate the amount of truncation of the in-phase stiffness by quick recovery during the length change. During maintained contraction in Ca^{2+}-containing media, the ratio of quadrature to in-phase stiffness, at Mg ATP concentrations above 400 μM, indicates that the sinusoidal tension signal was leading the length driver by a phase angle of approximately 20 deg. Assuming a single-exponential decay process associated with the observed phase lead, the magnitude of truncation of the in-phase component would be about 9%. However, additional more rapid exponential components could result in greater attenuation. Further quantitative analysis of the stiffness records was not undertaken since the contributions of end compliance, non-linearity and truncation were not determined in the experiments.

Relation between the mechanical and biochemical kinetics. The mechanical changes during activation have kinetic properties that are compatible with several of the main features of the transient kinetic studies of the myosin and actomyosin ATPases in solution (Taylor, 1979). These studies suggest that, at relatively low actin concentrations, the pathway of ATP hydrolysis catalysed by actomyosin involves ATP-induced actomyosin dissociation, ATP cleavage on myosin resulting in a myosin–products complex, recombination of the myosin–products complex to actin and, finally, dissociations of P_i and ADP resulting in free actomyosin that is now ready for another catalytic cycle. For these elementary steps only the ATP-induced actomyosin dissociation is expected to have a marked rate dependence on ATP concentration, the rate constant for this process being of the order 1×10^6 M^{-1} s^{-1} (White & Taylor, 1976; Goldman *et al.* 1984). The rate constant of the step controlling ATP cleavage is about 50–100 s^{-1} at 20 °C (Lymn & Taylor, 1971; Stein, Chock & Eisenberg, 1981). The reattachment rate of actin to a myosin–products complex is rapid (>500 s^{-1} at 44 μM-actin: Stein, Schwartz, Chock & Eisenberg, 1979). The rate of product release (20–40 s^{-1}) is presumed to be the rate-limiting step of the cycle (Weeds & Taylor, 1975; Mornet, Bertrand, Pantel, Audemard & Kassab, 1981), although the steady-state ATPase rate in isometrically contracting muscle fibres is an order of magnitude lower (Takashi & Putnam, 1979; Ferenczi *et al.* 1984). At higher actin concentrations an alternative pathway of ATP hydrolysis involves ATP cleavage on an actomyosin complex (Stein *et al.* 1979). In this case, ATP-induced actomyosin dissociation still occurs, but the mass-action effect causes the actomyosin–ATP intermediate to be more heavily populated. These pathways and the associated rate constants are compatible with the mechanical responses we have observed here. In particular, the absence of an effect of ATP concentration on the rate constant for reattachment or force generation is expected. It is possible that the observed reattachment rate constant (k_r) is controlled by the rate of the ATP cleavage step. However, it is

important to note that it is force generation, rather than reattachment, which has been recorded in the rising phase of the tension records, and this process may be controlled by a reaction involving an actomyosin–products complex.

Kinetic model. The shape of the tension transients initiated by photolysis of caged ATP has been qualitatively explained on the basis of rapid detachment of cross-bridges followed by reattachment. In order to determine if this hypothesis would lead naturally to the type of tension and stiffness records which have been obtained in this study, a simple kinetic simulation was conducted. The cross-bridge cycle was taken as follows:

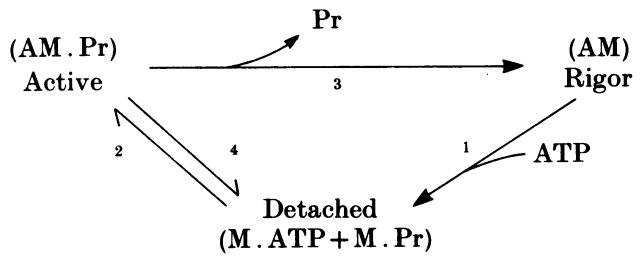

Scheme I

where M = myosin, A = actin, Pr = products of ATP hydrolysis (ADP and/or inorganic phosphate).

The simulation began with all cross-bridges in the rigor state. ATP liberated from caged ATP was considered to detach rigor cross-bridges (reaction 1) with a second-order rate constant given in the Appendix. In the presence of Ca^{2+} ions the cross-bridges were assumed to reattach to the thin filament and produce force in a first-order step (reaction 2). Attachment was considered reversible (reaction 4) and cycling with further ATP hydrolysis was allowed via reaction 3.

In order to simulate transient reattachment of cross-bridges in the absence of Ca^{2+}, cross-bridges were considered to interact co-operatively in pairs. In this case, reaction 2 was allowed to proceed for one detached cross-bridge of a pair only when its partner was attached to actin. If both cross-bridges were detached then further attachment was not allowed for that pair. In the presence of Ca^{2+}, cross-bridge attachment (reaction 2) was allowed regardless of the state of the partner, i.e. there was no co-operative behaviour. Otherwise all rate constants were the same in the presence and absence of Ca^{2+}. This simulation was similar to the model considered previously (Goldman *et al.* 1982; Hibberd, Goldman & Trentham, 1983), except that step 4 has been added and step 3 is much slower in the present calculation. Reactions in the presence of Ca^{2+} were not previously discussed. The differential equations describing the concentrations of each possible combination of two cross-bridges are listed in the Appendix. Thirteen simultaneous differential equations were solved using the Gear (1971) method. Further details of the calculation are given in the Appendix.

Fig. 7 shows the results of the kinetic simulation at two ATP concentrations (panel *A*, 500 μM-ATP; panel *B*, 250 μM-ATP). The traces simulate the mechanical response in the presence (+) and absence (−) of Ca^{2+}. The upper traces (Q) indicate the proportion of active cross-bridges in Scheme I. The central set of traces (S) represent the sum of all attached cross-bridges (rigor + active). The lowest set (T_a, T_b, T_c) simulates tension transients. Rigor cross-bridges were assigned a weight, relative to

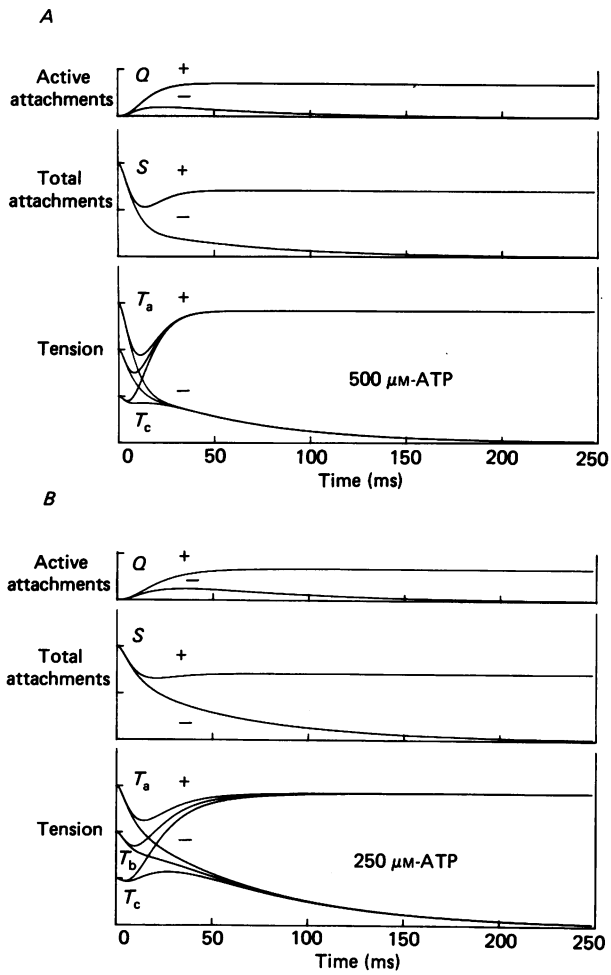

Fig. 7. Simulated stiffness and force transients from the model described in the text and Appendix. Initial myosin head concentration was 200 μM. Final released ATP concentrations were 500 μM (*A*) and 250 μM (*B*). Rate constants in text Scheme I: $k_1 = 8 \times 10^5$ M^{-1} s^{-1}; $k_2 = 100$ s^{-1}; $k_3 = 1{\cdot}5$ s^{-1}; $k_4 = 40$ s^{-1}. Traces labelled + and − simulate the presence and absence of Ca^{2+} respectively. *Q* traces represent active cross-bridges. *S* traces represent active and rigor cross-bridges. *T* traces represent active and rigor cross-bridges weighted as described in the Appendix.

the active cross-bridges. The weights of the rigor cross-bridges were altered before the start of the simulation, as in a pre-stretch or pre-release experiment.

The simulations resemble the experimental recordings of tension, stiffness and quadrature stiffness in many respects. Some of the similarities between this type of calculation and the experimental records obtained in the absence of Ca^{2+} have been described previously (Goldman *et al.* 1982; Hibberd *et al.* 1983). Here we note several important additional features. The amplitude of the transient tension increase was

enhanced when either initial rigor tension or the ATP concentration was low. The final phase of relaxation was less dependent on ATP concentration than the early parts of the transient. These phenomena are also characteristic of the experimental tension records (Goldman *et al.* 1984). The calculated total number of attachments (S) declined monotonically throughout the simulation although somewhat more rapidly than in the experimental stiffness traces (Fig. 2 and Goldman *et al.* 1984, Figs. 2 and 8). The number of active attachments (Q) increased after a delay and then decayed. This behaviour resembles the experimental quadrature stiffness recordings (Fig. 2 and Goldman *et al.* 1984, Fig. 8).

For the simulated high-Ca^{2+} transients (+), tension initially decreased below the level of the steady active force. The amplitude of the transient tension decrease was enhanced when either the initial rigor tension or the liberated ATP concentration was high. The time between the beginning of the simulation and the minimum tension was increased when either the initial rigor tension was high or the ATP concentration was low. These characteristics were also observed in the experimental records (Figs. 3 and 4).

The simulated proportion of attachments decreased from the rigor level (100 %) to a steady value given approximately by $100.k_2/(k_2+k_4)$. A transient decrease below the steady level occurred. These properties were observed in the experimental in-phase stiffness traces (Figs. 2, 3 and 4). However, as mentioned previously, contribution of non-linear end compliance to the final increase of stiffness in the experimental records has not been ruled out. The calculated number of active cross-bridges increased after a delay to a steady value. The simulation resembles the out-of-phase stiffness records (Figs. 2 and 4) although the + and − traces separated earlier in the simulation than in the experimental records.

We conclude from this kinetic simulation that the main features of our mechanical records can be explained on the basis of rapidly reattaching cross-bridges with few further assumptions. Certain aspects of this simulation do not correspond to the experimental records. The total number of cross-bridges (S) and the steady proportion of active cross-bridges (Q) in the simulated steady state change less than the experimental in-phase and quadrature stiffness records when ATP concentration is altered (cf. Figs. 4 and 7). The + and − simulated stiffness traces separate earlier than the corresponding experimental traces and the $-Ca^{2+}$ total number of cross-bridges decreases more rapidly than the experimental stiffness record. This model is highly simplified in a number of respects including neglect of stress or strain dependence on reaction rates and assuming co-operativity between only two cross-bridges. These and other simplifications contribute to the limitations of the model considered.

Implications for the physiological cross-bridge cycle

The high rate of cross-bridge detachment which occurs both in the presence and absence of Ca^{2+} indicates that neither ATP binding to the nucleotide-free cross-bridge nor detachment is a rate-limiting step in the over-all cross-bridge cycle, and they are not steps at which significant regulatory control is exerted. The apparent detachment rates observed in this study and in the previous paper (Goldman *et al.* 1984) ranged

up to 200 s^{-1}, and there was no evidence for saturation of this rate at ATP concentrations up to 1 mM. Thus the detachment reaction from the rigor state may be considerably faster under physiological conditions (5 mM-Mg ATP) than that observed in these experiments.

The reattachment rate of 50–100 s^{-1} is also markedly faster than the over-all cycling rate of cross-bridges as measured by the ATPase rate of muscle fibres (Curtin, Gilbert, Kretzschmar & Wilkie, 1974; Levy, Umazume & Kushmerick, 1976; Takashi & Putman, 1979; Ferenczi *et al.* 1984). In Scheme I, if reactions 1 and 2 are rapid compared to reaction 3, and reaction 4 is negligible, then cross-bridges would spend a high proportion of the cross-bridge cycle in the active force-generating state. For instance, with $k_1 = 200\ s^{-1}$, $k_2 = 70\ s^{-1}$ and $k_3 = 1{\cdot}5\ s^{-1}$, the cycling cross-bridges in a steady contraction would spend about 98% of the time in the active cross-bridge intermediate. Several studies indicate that the proportion of attached cross-bridges in active muscle fibres is lower. The intensity of equatorial X-ray reflexions indicates that in steady active contractions 60–90% of the cross-bridges are attached (Haselgrove & Huxley, 1973; Matsubara *et al.* 1975). Mechanical stiffness is lower during active contraction of a muscle fibre than in rigor (Goldman & Simmons, 1977; Yamamoto & Herzig, 1978). The orientation of nitroxide spin labels covalently bound to rabbit muscle fibres indicate a lower proportion of immobilized cross-bridges in active contractions compared to rigor (Cooke, Crowder & Thomas, 1982).

A simple change to the rate constants of the cross-bridge cycle, which reduces the proportion of attached cross-bridges and is consistent with the high measured rates of detachment and reattachment, is to make attachment reversible. In that case the reattachment reaction estimated as 50–100 s^{-1} from analysis of the experimental results would correspond to the sum of the attachment and reverse attachment steps ($k_2 + k_4$). The simulation shown in Fig. 7 was conducted with a reversible attachment reaction. Another possible factor which might cause a significant proportion of cross-bridges to be detached during a contraction is the difference in repeat periodicities of the thick and thin filaments (H. E. Huxley & Brown, 1967). Filament lattice geometry might cause a proportion of the myosin heads to be excluded from the cross-bridge cycle. In this case the reaction rates we measure would pertain only to those cross-bridges which were cycling and splitting ATP. Other pathways of the reaction, such as a side branch which allows rapid detachment of the cross-bridges in the absence of Ca^{2+}, would also be consistent with the experiments. At present, the data do not allow us to distinguish these possibilities.

The rapid reattachment of cross-bridges observed in the present experiments suggests that little control of the cross-bridge cycle or rate limitation could occur in intermediate steps while the cross-bridges are detached. Thus suggestions of a detached rate limitation due to a 'refractory state' of detached cross-bridges seem unlikely on the basis of the present experiments. We conclude that a slow step between the reaction leading to force generation and the binding of ATP by a cross-bridge controls the over-all cycling rate in a fully active isometric contraction.

APPENDIX

The method for calculation of simulated mechanical transients during contraction or relaxation initiated by a step increase in ATP concentration is described in this section. Pairs of cross-bridges are considered to interact to simulate co-operativity of attachment in the absence of Ca^{2+}. Let the cross-bridge cycle correspond to Scheme I of the Discussion with the following notation:

P = primary rigor cross-bridge present at the time of liberation of ATP,
N = detached cross-bridge,
A = actively force-generating cross-bridge,
S = secondary rigor cross-bridge (formed by product release from A),
T = ATP,
D = ADP,
CT = caged ATP.

The possible combinations of pairs of cross-bridges are PP, PN, PA, PS, NN, NA, NS, AA, AS and SS. Note that pairs with reversed states, such as PN and NP, are considered identical. The system of differential equations describing the reactions is:

	Detachment	Attachment	Product release	Reverse attachment	Ca^{2+}-depen attachment
$PP]/dt$	$=-2k_1[T][PP]$				
$PN]/dt$	$=+k_1[T](2[PP]+[PS]-[PN])$	$-k_2[PN]$		$+k_4[PA]$	
$PA]/dt$	$=-k_1[T][PA]$	$+k_2[PN]$	$-k_3[PA]$	$-k_4[PA]$	
$PS]/dt$	$=-2k_1[T][PS]$		$+k_3[PA]$		
$NN]/dt$	$=+k_1[T]([PN]+[NS])$			$+k_4[NA]$	$-2k_5[NN]$
$NA]/dt$	$=+k_1[T]([PA]+[AS])$	$-k_2[NA]$	$-k_3[NA]$	$+k_4(2[AA]-[NA])$	$+2k_5[NN]$
$NS]/dt$	$=+k_1[T](2[SS]+[PS]-[NS])$	$-k_2[NS]$	$+k_3[NA]$	$+k_4[AS]$	
$AA]/dt$	$=$	$+k_2[NA]$	$-2k_3[AA]$	$-2k_4[AA]$	
$AS]/dt$	$=-k_1[T][AS]$	$+k_2[NS]$	$+k_3(2[AA]-[AS])$	$-k_4[AS]$	
$SS]/dt$	$=-2k_1[T][SS]$		$+k_3[AS]$		

$$T]/dt = -k_1[T](2[PP]+[PN]+[PA]+[PS]+2[SS]+[NS]+[AS]+[PS])+k_6[CT]+k_7[D]$$
$$D]/dt = -k_7[D] + k_3(2[AA]+[NA]+[PA]+[AS])$$
$$CT]/dt = -k_6[CT]$$

For the simulations shown in Fig. 7 the initial concentrations of the reactants were all zero except [CT] = 500 μM (panel *A*) or 250 μM (*B*) and [PP] = 100 μM simulating 200 μM-myosin heads in rigor. The reaction rate constants were:

$k_1 = 8 \times 10^5$ M^{-1} s^{-1}; ATP-induced detachment rate of rigor cross-bridges,
$k_2 = 100$ s^{-1}; cross-bridge attachment rate,
$k_3 = 1{\cdot}5$ s^{-1}; product release rate,
$k_4 = 40$ s^{-1}; reverse attachment rate,

$$k_5 = \left\{\begin{matrix}100\text{ s}^{-1}\text{ in the presence of Ca}^{2+}\\ 0\text{ s}^{-1}\text{ in the absence of Ca}^{2+}\end{matrix}\right\} \left\{\begin{matrix}\text{cross-bridge attachment rate for each}\\ \text{cross-bridge when both cross-bridges}\\ \text{of a pair are detached,}\end{matrix}\right.$$

$k_6 = 100$ s^{-1}; release of ATP rate from caged ATP,
$k_7 = 10$ s^{-1}; rate of rephosphorylation of ADP to ATP by creatine kinase.

The thirteen simultaneous equations were integrated by the Gear (1971) method

incorporated into a reaction simulation computer program (Stabler & Chesick, 1978) and implemented on a Z-80 based computer. The computer output gave the concentration of each of the ten cross-bridge pair types along with [T], [D] and [CT] as functions of time. In order to plot the simulated traces shown in Fig. 7 the following relative weights were assigned to each cross-bridge state:

	Weights			
Trace	C_P	C_N	C_A	C_S
Q	0	0	1	0
S	1	0	1	1
T_a	0·75	0	1	1
T_b	0·5	0	1	1
T_c	0·25	0	1	1

where C_P, C_N, C_A and C_S are weighting coefficients for the cross-bridge states. The weighted sum:

$$W = C_P[P] + C_N[N] + C_A[A] + C_S[S]$$

was calculated including individual cross-bridges irrespective of the state of their partner. W was plotted *vs.* time to simulate the experiments. Reaction rates were considered to be independent of stress or strain. Only the primary (original) rigor bonds were given weights other than 0 or 1·0. The + and − Ca^{2+} simulated traces were calculated with all rate constants identical except k_5 for the reaction:

$$NN \xrightarrow{2k_5} NA$$

which occurred only in the presence of Ca^{2+}.

We are grateful to Ms Jody Dantzig for expert assistance and helpful discussions, Mr Miles J. Gessow and Mrs Fanny Itshak for skilled technical assistance and Mrs Joan Loepp for preparation of the manuscript. The work was supported by grants from the NIH (HL 15835 to the Pennsylvania Muscle Institute, and AM 00745). M.G.H. was a British–American Research Fellow of the American Heart Association and the British Heart Foundation.

REFERENCES

CECCHI, G., GRIFFITHS, P. J. & TAYLOR, S. (1982). Muscular contraction: kinetics of crossbridge attachment studied by high-frequency stiffness measurements. *Science* **217**, 70–72.

COOKE, R., CROWDER, M. S. & THOMAS, D. D. (1982). Orientation of spin labels attached to cross-bridges in contracting muscle fibres. *Nature* **300**, 776–778.

CURTIN, N. A., GILBERT, C., KRETZSCHMAR, K. M. & WILKIE, D. R. (1974). The effect of the performance of work on total energy output and metabolism during muscular contraction. *Journal of Physiology* **238**, 455–472.

EISENBERG, E., HILL, T. L. & CHEN, Y. (1980). Cross-bridge model of muscle contraction. Quantitative analysis. *Biophysical Journal* **29**, 195–227.

FERENCZI, M. A., HOMSHER, E. & TRENTHAM, D. R. (1984). The kinetics of magnesium adenosine triphosphate cleavage in skinned muscle fibres of the rabbit. *Journal of Physiology* **352**, 575–599.

FORD, L. E., HUXLEY, A. F. & SIMMONS, R. M. (1977). Tension responses to sudden length change in stimulated frog muscle fibres near slack length *Journal of Physiology* **269**, 441–515.

GEAR, C. W. (1971). *Numerical Initial Value Problems in Ordinary Differential Equations*, chap. 11. New Jersey: Prentice-Hall.

GOLDMAN, Y. E., HIBBERD, M. G., MCCRAY, J. A. & TRENTHAM, D. R. (1982). Relaxation of muscle fibres by photolysis of caged ATP. *Nature* **300**, 701–705.

GOLDMAN, Y. E., HIBBERD, M. G. & TRENTHAM, D. R. (1984). Relaxation of rabbit psoas muscle fibres from rigor by photochemical generation of adenosine-5′-triphosphate. *Journal of Physiology* **354**, 577–604.

GOLDMAN, Y. E. & SIMMONS, R. M. (1977). Active and rigor muscle stiffness. *Journal of Physiology* **269**, 55–57*P*.

HASELGROVE, J. C. & HUXLEY, H. E. (1973). X-ray evidence for radial cross-bridge movement and for the sliding filament model in actively contracting skeletal muscle. *Journal of Molecular Biology* **77**, 549–568.

HIBBERD, M. G., GOLDMAN, Y. E. & TRENTHAM, D. R. (1983). The mechanical response of muscle fibers to a rapid increase in concentration of ATP. In *Biological Structures and Coupled Flows*, ed. OPLATKA, A. & BALABAN, M., pp. 223–238. New York: Academic Press.

HUXLEY, A. F. (1957). Muscle structure and theories of contraction. *Progress in Biophysics and Biophysical Chemistry* **7**, 255–318.

HUXLEY, A. F. (1974). Muscular contraction. *Journal of Physiology* **243**, 1–43.

HUXLEY, H. E. (1979). Time resolved X-ray diffraction studies on muscle. In *Cross-bridge Mechanism in Muscle Contraction*, ed. SUGI, H. & POLLACK, G. H., pp. 391–405. Tokyo: University of Tokyo Press.

HUXLEY, H. E. & BROWN, W.(1967). The low-angle X-ray diagram of vertebrate striated muscle and its behaviour during contraction and rigor. *Journal of Molecular Biology* **30**, 383–434.

JULIAN, F. J., SOLLINS, K. R. & SOLLINS, M. R. (1974). A model for the transient and steady-state mechanical behavior of contracting muscle. *Biophysical Journal* **14**, 546–562.

KAWAI, M. & BRANDT, P. W. (1980). Sinusoidal analysis: a high resolution method for correlating biochemical reactions with physiological processes in activated skeletal muscles of rabbit, frog and crayfish. *Journal of Muscle Research and Cell Motility* **1**, 279–303.

LEVY, R. M., UMAZUME, Y. & KUSHMERICK, M. J. (1976). Ca^{2+} dependence of tension and ADP production in segments of chemically skinned muscle fibers. *Biochimica et biophysica acta* **430**, 352–365.

LYMN, R. W. & TAYLOR, E. W. (1971). Mechanism of adenosine triphosphate hydrolysis by actomyosin. *Biochemistry* **10**, 4617–4624.

MATSUBARA, I. & YAGI, N. (1978). A time-resolved X-ray diffraction study of muscle during twitch. *Journal of Physiology* **278**, 297–307.

MATSUBARA, I., YAGI, N. & HASHIZUME, H. (1975). Use of an X-ray television for diffraction of the frog striated muscle. *Nature* **255**, 728–729.

MCCALLA, T. R. (1967). *Introduction to Numerical Methods and FORTRAN Programming*. New York: Wiley.

MORNET, D., BERTRAND, R., PANTEL, P., AUDEMARD, E. & KASSAB, R. (1981). Structure of the actin–myosin interface. *Nature* **292**, 301–306.

PODOLSKY, R. J. & NOLAN, A. C. (1973). Muscle contraction tansients, cross-bridge kinetics, and the Fenn effect. *Cold Spring Harbor Symposia on Quantitative Biology* **37**, 661–668.

STABLER, R. N. & CHESICK, J. P. (1978). A program system for computer integration of multistep reaction rate equations using the Gear integration method. *International Journal of Chemical Kinetics* **10**, 461–469.

STEIGER, G. J. & ABBOTT, R. H. (1981). Biochemical interpretation of tension transients produced by a four-state mechanical model. *Journal of Muscle Research and Cell Motility* **2**, 245–260.

STEIN, L. A., CHOCK, P. B. & EISENBERG, E. (1981). Mechanism of the actomyosin ATPase: effect of actin on the ATP hydrolysis step. *Proceedings of the National Academy of Sciences of the U.S.A.* **78**, 1346–1350.

STEIN, L. A., SCHWARZ JR, R. P., CHOCK, P. B. & EISENBERG, E. (1979). Mechanism of actomyosin adenosine triphosphatase. Evidence that adenosine-5′-triphosphate hydrolysis can occur without dissociation of the actomyosin complex. *Biochemistry* **18**, 3895–3909.

TAKASHI, R. & PUTNAM, S. (1979). A fluorimetric method for continuously assaying ATPase: application to small specimens of glycerol-extracted muscle fibers. *Analytical Biochemistry* **92**, 375–382.

TAYLOR, E. W. (1979). Mechanism of actomyosin ATPase and the problem of muscle contraction. *Chemical Rubber Company Critical Reviews of Biochemistry* **6**, 103–164.

THORSON, J. & WHITE, D. C. S. (1983). Role of cross-bridge distortion in the small-signal mechanical dynamics of insect and rabbit striated muscle. *Journal of Physiology* **343**, 59–84.

WEEDS, A. G. & TAYLOR, R. S. (1975). Separation of subfragment-1 isoenzymes from rabbit skeletal muscle myosin. *Nature* **257**, 54–56.

WHITE, H. D. & TAYLOR, E. W. (1976). Energetics and mechanism of actomyosin adenosine triphosphatase. *Biochemistry* **15**, 5818–5826.

YAMAMOTO, T. & HERZIG, J. W. (1978). Series elastic properties of skinned muscle fibres in contraction and rigor. *Pflügers Archiv* **373**, 21–24.